Liver INTERNATIONAL
OFFICIAL JOURNAL OF THE INTERNATIONAL ASSOCIATION FOR THE STUDY OF THE LIVER

Liver International ISSN 1478-3223

CLINICAL STUDIES

Heterogeneous nuclear ribonucleoprotein A2/B1 in association with hTERT is a potential biomarker for hepatocellular carcinoma

Hideki Mizuno[1], Masao Honda[1,2], Takayoshi Shirasaki[1,2], Taro Yamashita[1], Tatsuya Yamashita[1], Eishiro Mizukoshi[1] and Shuichi Kaneko[1]

1 Department of Gastroenterology, Kanazawa University Graduate School of Medicine, Kanazawa, Japan
2 Department of Advanced Medical technology, Kanazawa University Graduate School of Health Medicine, Kanazawa, Japan

Keywords
HCC – hnRNP A2/B1 – hTERT

Abbreviations
HCC, hepatocellular carcinoma; hnRNP A2/B1, heterogeneous nuclear ribonucleoprotein A2/B1; hTERC, human telomerase RNA component; hTERT, human telomerase reverse transcriptase subunit; TRAP, telomere repeat amplification protocol.

Correspondence
Masao Honda, Department of Gastroenterology, Graduate School of Medicine, Kanazawa University, Takara-machi 13-1, Kanazawa 920-8641, Japan
Tel: +81 76 265 2235
Fax: +81 76 234 4250
e-mail: mhonda@m-kanazawa.jp

Received 31 August 2011
Accepted 2 February 2012

DOI:10.1111/j.1478-3231.2012.02778.x

Abstract

Background: The heterogeneous nature of hepatocellular carcinoma (HCC) and the lack of appropriate biomarkers have hampered patient prognosis and treatment stratification. To identify a new prognostic biomarker that is related to human telomerase reverse transcriptase (hTERT) in HCC, we employed a unique proteomics approach using liquid chromatograph-mass spectrometry/mass spectrometry (LC-MS/MS) after gel filtration purification of liver tissue. *Methods:* Protein lysates from HCC and cirrhotic liver tissue were subjected to gel filtration using high performance liquid chromatography. The telomerase complex was identified at a molecular mass of 350 kDa in parallel with telomerase activity. These fractionated lysates of 350 kDa were analyzed by LC-MS/MS. The relation of the identified marker and prognosis was statistically examined in surgically resected HCC patients. *Results:* We identified 24 differentially expressed proteins in HCC. One of these proteins, heterogeneous nuclear ribonucleoprotein A2/B1 (hnRNP A2/B1), was further analyzed by immunoprecipitation assay using tissue and cell line samples and found to interact with hTERT. Moreover small interfering RNA against hnRNP A2/B1 suppressed telomerase activity, and immunohistochemical examination showed that the enhanced nuclear and cytoplasmic hnRNP A2/B1 expression in HCC was significantly associated with histological grade of tumor differentiation and microvascular invasion of HCC. Furthermore, survival analysis of 74 HCC patients who received curative surgical treatment showed that hnRNP A2/B1 expression is an independent prognostic factor for patient survival. *Conclusions:* Heterogeneous nuclear ribonucleoprotein A2/B1, an hTERT-associated protein, is a potential prognostic biomarker for HCC patients and might be a therapeutic target of HCC.

Hepatocellular carcinoma (HCC) has extremely poor prognosis and remains one of the most aggressive human malignancies worldwide(1, 2). The high mortality associated with this disease can be attributed mainly to the inability to diagnose HCC patients at an early stage. Currently, α-fetoprotein (AFP) and protein induced by vitamin K absence or antagonists-II (PIVKA-II) are serologic biomarkers for HCC in clinical practice. However, the sensitivity of these markers is not adequate, and a nonspecific elevation in cirrhotic liver is frequently observed. Furthermore, there is an urgent need to identify additional diagnostic as well as prognostic biomarkers of HCC.

Telomerase is a ribonucleoprotein complex that maintains chromosome stability and cell lifespan by telomere maintenance(3–5). The minimal components of active telomerase include human telomerase reverse transcriptase (hTERT), the catalytic subunit, and its template RNA (hTERC) that encodes the template for synthesizing telomeric DNA(6, 7). Various host factors are associated with telomerase and maintain the homeostasis of telomeres(8). Although direct evaluation of protein expression of hTERT would be clinically useful, measurement of hTERT expression in tissue samples is less sensitive and unreliable due to the limitation of appropriate hTERT antibody(9). It would be ideal if some of the hTERT-associated proteins were closely linked to telomerase activity as this could function as a useful biomarker of tumor growth, invasion, and metastasis of HCC.

The aim of this study was to identify a new prognostic biomarker of HCC which was related to hTERT. By employing a proteomics approach combined with gel-filtration protein purification method, we found that the heterogeneous nuclear ribonucleoprotein (hnRNP)

A2/B1 was associated with hTERT and would be a useful prognostic marker of HCC.

Materials and methods

Tissue collection and preparation

All HCC and adjacent cirrhotic (non-cancerous) liver tissue samples were obtained from 74 patients who underwent surgical resection between 2000 and 2009 at Kanazawa University Hospital, Kanazawa, Japan. Follow-ups were terminated in February, 2011. The median follow-up was 38 months (range, 2–83 months). Follow-up data of clinical, aetiological, histological, imaging (ultrasonography, contrast-enhanced helical computed tomography, and magnetic resonance imaging), and treatment details were collected prospectively and added to a customized database as soon as an event such as surgery, follow-up, or death occurred.

Liver tissue samples were formalin-fixed, paraffin-embedded, and used for immunohistochemistry. Histological characterization of HCC and adjacent cirrhotic liver was performed according to the Classification of the Liver Cancer Study Group of Japan and the method described by Desmet *et al.*(10).

For proteomics analysis, three HCC and adjacent cirrhotic liver tissue samples were snap-frozen and stored in liquid nitrogen until later use in gel filtration. Three patients for proteomics analysis belong to the group of 74 patients who underwent surgical resection and were followed-up. The characteristics of these patients were described previously (patients Nos. 4, 8, and 10). All three were positive for Hepatitis C virus (HCV) antibody, and histological examination of HCC was moderately differentiated in two patients and poorly differentiated in one patient(11).

The study was approved by the appropriate ethics committees and the institutional review boards at Kanazawa University and complied with Good Clinical Practice Guidelines, the Declaration of Helsinki, and local laws and regulations.

Preparation of protein lysates and gel filtration of protein lysates

Hepatocellular carcinoma and adjacent cirrhotic liver tissue (100 mg) were ground into powder, homogenized in CelLytic™ MT (detergent, bicine, and 150 mM NaCl; Sigma-Aldrich, St Louis, MO,USA), and sonicated. Protein lysates from the tissue specimens were independently fractionated on HiLoad 16/60 Superdex 200 pg gel filtration columns using a high-performance liquid chromatography (HPLC) system (GE Healthcare, Buckinghamshire, England, UK), which provides rapid screening, method scouting, method optimization, and scale-up experiments, in CelLytic™ MT (Sigma-Aldrich). The resulting fractions were resolved by sodium dodecyl sulfate polyacrylamide gel electrophoresis (SDS-PAGE), probed with various antibodies, and used for proteomic study by liquid chromatograph-mass spectrometry/mass spectrometry (LC-MS/MS). The column was calibrated with a high molecular weight calibration kit (HMW Native Marker Kit; GE Healthcare).

Protein identification by mass spectrometry

Protein-fractionated lysates were carbamidomethylated by 6M Urea, 500 mM Tris–HCL, 2.5 mM EDTA, and 250 mM iodoacetamide and digested with 100 ng/uL trypsin. Peptide mixtures were redissolved in 0.5% trifluoroacetic acid (TFA), and 1 μg of the peptide solution was mixed with 1 μL of matrix (4-hydroxy-α-cyanocinnamic acid in 30% ACN, 0.1% TFA) before spotting on a target plate. The digested peptides were analyzed by a Hitachi Liquid Chromatograph Mass Spectrometer coupled to a Q-TOF Mass Spectrometer (NanoFrontier eLD; Hitachi High-Technologies Co. Ltd., Tokyo, Japan). The acquired MS/MS spectra were searched for in Swiss-Prot using the Mascot search engine (Matrix Sciences, London, UK). Search parameters were set as follows: peptide mass tolerance, ± 0.3 Da; MS/MS ion mass tolerance, ± 0.3 Da; and trypsin for the enzyme set. The proteins were identified using a P value of ≤ 0.05 and Mascot scores of >35 were considered as promising hits. The mean expression ratio of in HCC to proteins identified in adjacent cirrhotic liver tissue was calculated, and a difference of more than two-fold was used as a filtering criterion.

Immunoprecipitation of protein lysates

The protein lysates were incubated at 4°C for 3 h with 10 μL of GammaBind G resin containing prebound anti-FLAG M2 (Sigma–Aldrich) or anti-hnRNP A2/B1 (Abcam, Cambridge, UK), followed by three washes with CelLytic™ MT (Sigma-Aldrich). These bound proteins were separated by SDS-PAGE and visualized by western blotting.

Plasmid construction

The FLAG-GST retrovirus expression vector pBabe-puro-FLAG-GST was constructed by inserting the *FbaI-XhoI* fragment of FLAG-GST cDNA into the *BamHI-SalI* site of the pBabe-puro vector. The GST cDNA of pBabe-puro-FLAG-GST was replaced by the *EcoRI-SalI* fragment containing hTERT cDNA and resulted in retrovirus delivery vector pBabe-puro-FLAG-hTERT(12).

Mammalian cell lines and retrovirus delivery

Huh7 (human hepatocellular carcinoma cell line) and 293T cells (human kidney cell line) were cultured by standard methods in Dulbecco's modified Eagle's med-

ium (DMEM; Gibco BRL, Gaithersburg, MD, USA) supplemented with 10% fetal bovine serum (FBS) and 1% penicillin/streptomycin. Recombinant retrovirus packaging, infection, and selection of FLAG-hTERT expressing stable transformations of Huh7 cells were preformed as described(13).

Preparation of cell lysates and immunoprecipitation

Cells were harvested, washed with phosphate buffered solution (-) and sonicated in CelLytic™ M (SigmaAldrich). Lysates of 5 × 10(6) cells were diluted 10-fold in CelLytic™ M and incubated at 4°C for 3 h with 10 μL of GammaBind G resin containing prebound anti-FLAG M2 or anti-hnRNP A2/B1, followed by three washes with CelLytic™ M. The bound proteins were separated by SDS-PAGE and visualized by western blotting.

Antibodies and western blot analysis

For western blot analysis, total cell lysates and their fractions from gel filtration were separated by SDS-PAGE and transferred to a nitrocellulose membrane then probed with anti-hTERT (Rockland Inc., Gilbertsville, PA, USA), anti-Hsp90α/β (Santa Cruz Biotechnology, CA, USA), anti-hnRNP A2/B1 (Abcam), anti-FLAG M2 (Sigma-Aldrich), or anti-β-actin (Sigma-Aldrich) primary antibodies, followed by incubation with horseradish peroxidase conjugated goat anti-mouse immunoglobulin (Ig) G secondary antibody (Amersham Biosciences, Buckinghamshire, England, UK) for anti-Hsp90α/β, anti-hnRNP A2/B1, anti-FLAG M2, and anti-β-actin antibodies or horseradish peroxidase conjugated goat anti-Rabbit IgG secondary antibody (Thermo Scientific, Rockford, IL, USA) for anti-hTERT antibody. Densitometric analysis was conducted directly on the blotted membrane using a CCD camera (LAS-3000 Mini; Fujifilm, Tokyo, Japan) and Scion Image software.

Small interfering RNA synthesis

Small interfering (si) RNA specific to hnRNP A2/B1 (HNRNPA2B1 siGENOME set) and the siGENOME Controls Basic kit were obtained from Thermo Scientific. To each well of a six-well plate, 2 × 10^5 Huh7 cells were seeded 12 h before transfection. Transfection was preformed using TransMessenger™ Transfection Reagent (Qiagen, West Sussex, UK) according to the manufacturer's protocol. A total of 100 pmol/L of siRNA duplex was used for each transfection.

Real-time quantitative reverse-transcription PCR

Real-time quantitative reverse-transcription polymerase chain reaction (RT-PCR) was performed for hnRNP A2/B1 using the ABI Prism 7900HT Sequence Detection System (Applied Biosystems, San Francisco, CA, USA). Primers and the TaqMan probe for hnRNP A2/B1were designed using the primer design software Primer Express™ (Applied Biosystems). The probe was labeled with a reporter fluorescent dye (6-carboxy-fluorescein) at the 5′ end and a quencher fluorescent dye (6-carboxy-tetramethyl-rhodamine) at the 3′ end. PCR conditions were 1 cycle at 50°C for 2 min and 95°C for 10 min, followed by 40 cycles at 95°C for 15 s and 60°C for 1 min. The level of messenger RNA (mRNA) expression relative to the internal control (β-actin) was calculated.

Telomerase activity assay

Telomerase activity was measured by a PCR-based telomere repeat amplification protocol (TRAP) enzyme-linked immunosorbent assay (ELISA). Telomerase activity was quantitatively measured using a TRAPEZE ELISA telomerase detection kit (MILLIPORE, Billerica, MA, USA) according to the manufacturer's protocol.

Immunohistochemical analysis

Paraffin-embedded sections of tissue blocks were orderly rehydrated to xylene and sequential alcohols, washed, and blocked by incubating slides in 0.6% hydrogen peroxide. The sections were treated with a 1:100 diluted solution of anti-hnRNP A2/B1 antibody for 30 min in a wet incubation box. Detection of the antibody was processed according to the manufacturer's protocol using Envision+ kits (Dako, Carpinteria, CA, USA). Slides were counterstained with hematoxylin for 30 s, dehydrated reversibly using sequential alcohols and xylene, and mounted with a coverslip using Histomount. Photographs for stained tissue section were captured using an Olympus DP70 CCD camera with an Olympus AX80 microscope (Olympus, New York, NY, USA).

Statistical analysis

The student's *t*-test was used to determine the statistical significance of the difference in cell viability between the two groups. The chi-square test was used to evaluate the correlation between clinicopathological characteristics and nuclear and cytoplasmic hnRNP A2/B1 expression. Univariate and multivariate Cox proportional hazards regression analysis was used to evaluate the association of nuclear and cytoplasmic hnRNP A2/B1 expression and clinicopathological parameters with patient outcome. All statistical analysis was performed using SPSS software (SPSS software package; SPSS Inc., Chicago, IL, USA).

Results

Fractionation of protein lysates from hepatocellular carcinoma and cirrhotic liver tissue

Protein lysates from HCC and cirrhotic liver tissue from patients were independently subjected to gel filtration

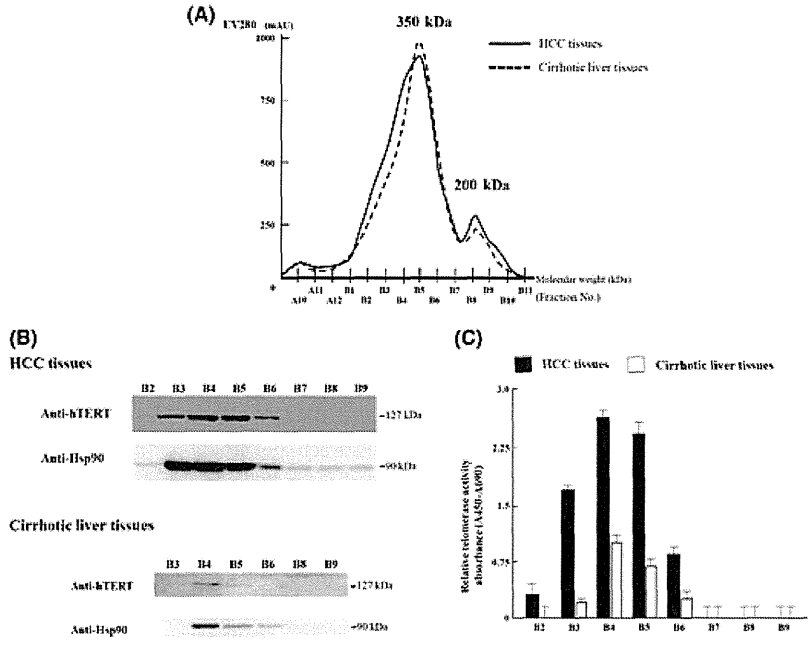

Fig. 1. Fractionation of protein lysates from HCC and cirrhotic liver tissue. (A) Protein lysates from HCC and cirrhotic liver tissues from three patients were fractionated on a 200 pg gel filtration column by high-performance liquid chromatography (HPLC). Mean values were drawn in the same axis. (B) Representative image of quantitative measurement of human telomerase reverse transcriptase (hTERT) protein and Hsp90 protein by western blotting with respective antibodies. (C) Relative telomerase activity of fractions measured by telomere repeat amplification protocol enzyme-linked immunosorbent assay.

by HPLC (Fig. 1A). Two peaks, corresponding to the molecular weights 350 kDa and 200 kDa in the fractionated proteins were found. Interestingly, hTERT was detected around the 350-kDa peak (Fraction Nos. B3–B6) concurrently with telomerase activity (Fig. 1B, 1C). Moreover Hsp90 was broadly distributed in two peaks of around 350 kDa and 200 kDa (Fraction Nos. B2–B9). The expression of hTERT by western blotting was higher (mean, five-fold) in HCC tissue than that in cirrhotic nodule tissue (Fig. 1B), and the telomerase activity quantified by TRAP ELISA was significantly higher (>2.5-fold) in HCC than in cirrhotic nodule tissue (Fig. 1B, 1C).

Identification of differentially expressed proteins

To discover hTERT-related proteins, we further analyzed the fractionated lysates of the 350-kDa peak (Fraction No. B4) from HCC and cirrhotic liver tissue by LC-MS/MS. After searching the MASCOT database (http://www.matrixscience.com), 144 proteins were selected according to identification criteria (see Materials and methods), and 24 of all identified proteins displayed more than a two-fold expression difference. Among these 24 proteins, eight were found to be up-regulated in HCC tissue compared with cirrhotic liver tissue, while 16 proteins were found to be down-regulated (Table 1). Of the 24 proteins, nine were already known as HCC-related proteins(14–20). To identify a new prognostic biomarker related to hTERT, we decided to focus on hnRNP A2/B1, which has been reported as a prognostic biomarker for lung cancer(21) and gastric cancer(22).

Validation of heterogeneous nuclear ribonucleoprotein A2/B1 expression and interaction with human telomerase reverse transcriptase subunit

To confirm the altered expression of hnRNP A2/B1 in HCC and non-cancerous liver, western blot analysis was performed with anti-hnRNP A2/B1 antibody. Both of hnRNP A2/B1 expression was detected around 350 kDa (Fraction Nos. B3–B7). The hnRNP A2/B1 protein level was higher in HCC tissue than that in non-cancerous liver tissue (Fig. 2A). To examine whether hnRNP A2/B1 can interact with hTERT, we performed an immunoprecipitation assay. hnRNP A2/B1-immunoprecipitates, derived from fractionated lysates of 350 kDa (Fraction No. B4) contained hTERT (Fig. 2B). However, in a reverse immunoprecipitation experiment, anti-hnRNP A2/B1 antibody was unable to recognize the hTERT protein band in hTERT-immunoprecipitates (data not shown). Therefore, we established Huh7 cells derived from stable cell lines that consistently expressed FLAG-tagged hTERT (see Materials and methods). hnRNP A2/B1-immunoprecipitates contained FLAG-hTERT, and

Table 1. Proteins identified by LC-MS/MS as significantly changed in expression between HCC tissues and cirrhotic nodule tissue[18–24]

Accession no.	Protein name	Molecular function	Protein ratio (HCC/cirrhotioc liver)
Up-regulated proteins in HCC tissue			
P 40925	Malate dehydrogenase	L-malate dehydrogenase activity, malic enzyme activity	2.38
Q 13228	*Selenium-binding protein 1*	*Protein binding, selenium binding*	2.07
P 22626	Heterogeneous nuclear ribonucleo protein in A2/B1	RNA binding, nucleotide binding	2.01
Q 13535	Serine/threonine-protein kinase ATR	ATP binding, DNA binding	1.92
Q 5T4S7	Zinc finger UBRl-type protein 1	Ubiquitin-protein in ligase activity, zinc ion binding	1.61
P 07335	Annexin A2	Calcium ion binding, cytoskeletal protein binding	1.53
P 30038	Delta-l-pyrroline-5-carboxylate dehydrogenase	1-pyrroline-5-carboxylate dehydrogenase activity	1.52
P 09651	Heterogeneous nuclear ribonucleo protein A1	RNA binding, nucleotide binding	1.48
Down-regulated proteins in HCC tissue			
Q 8NF91	Nesprin-1	Actin binding, lam in binding	0.67
P 00352	Retinal dehydrogenase 1	Ras GTPase activator activity	0.55
P 24752	Acetyl-coA acetyl transferase	Acetyl-coA acetyl transferase activity	0.51
P 00441	Superoxide dismutase (Cu-Zn)	C haperone binding copper ion binding	0.45
P 02787	Serotransfeirn recursor	Ferric ion binding	0.45
Q 8TE73	Ciliaary dyne in heavy chain 5	ATP binding, ATPase actvity	0.43
P 07327	Alcohol dehydrogenase 1A	Alcohol dehydrogenase activity (Zinc-dependent)	0.41
P 68871	Hemoglobnin subunit beta	Heme binding, hemoglobin binding, oxygen binding	0.39
Q 6PIU 2	Liver carboxyl esterase 1 precursor	Carboxyl esterase activity	0.38
Q 06830	Peroxiredoxin-1	Protein binding,thioredoxin peroxidase activity	0.36
P 69905	Hemoglobin subunit alpha	Heme binding, oxygen binding,	0.34
P 36871	Phosphoglucomutase-1	*Magnesium ion binding*	0.32
P 05089	Arginase-1	Arginase activity	0.32
P 30041	Peroxiredoxin-6	Glutathione peroxidase activity	0.29
P 00326	Alcohol dehydrogenase 1C	Alcoholdehydrogenase (NAD) activity	0.21
P 08319	Alcohol dehydrogenase 4	NAD binding, NADPH quinone reductase activity	0.15

ATP, adenosine 5'-triphosphate; GTP, guanosine triphosphate; HCC, hepatocellular carcinoma; NAD, nicotinamide adenine dinucleotide; NADPH, nicotinamide adenine dinucleotide phosphate-oxidase.

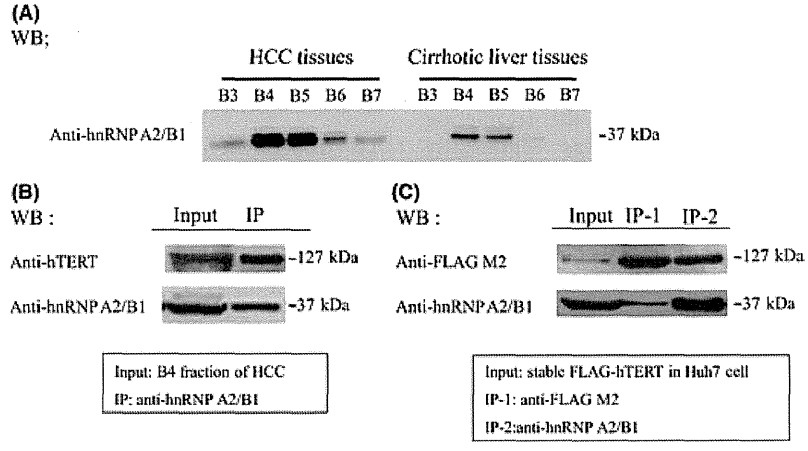

Fig. 2. Validation of hnRNP A1/B2. (A) Representative image of quantitative measurement of hnRNP A2/B1 protein by western blotting with anti-hnRNP A2/B1 antibody. (B) B4 fractionated lysates of HCC were immunoprecipitated with anti-hnRNP A2/B1 antibody. The bound proteins were separated by 8% sodium dodecyl sulfate polyacrylamide gel electrophoresis (SDS-PAGE) and subjected to western blotting with anti-hTERT and anti-hnRNP A2/B1 antibodies as indicated. The B4 fractionated lysates of HCC shown in the input correspond to 5% of the sample. (C) Total cell lysates from Huh7 cells stably expressing FLAG-hTERT were immunoprecipitated with anti-FLAG M2 (IP-1) and anti-hnRNP A2/B1 (IP-2) antibodies. The bound proteins were separated by 8% SDS-PAGE and subjected to western blotting using anti-FLAG M2 and anti-hnRNP A2/B1 antibodies as indicated. Total cell lysates shown in the input correspond to 5% of the sample.

Liver International (2012)

anti-hnRNP A2/B1 antibody recognized the FLAG-hTERT protein band in FLAG-M2 immunoprecipitates (Fig. 2C). These results confirmed that hnRNP A2/B1 can interact with hTERT.

Functional relevance of heterogeneous nuclear ribonucleoprotein A2/B1 expression on telomerase activity

To examine the functional relevance of hnRNP A2/B1 on hTERT activity, we performed knockdown of hnRNP A2/B1. Expression of hnRNP A2/B1 in Huh7 cells was significantly knocked down to 30–40% of the control using hnRNP A2/B1-specific siRNA (siGENOME, Thermo Scientific) (Fig. 3A). Under these conditions, the results of TRAP ELISA showed that telomerase activity was repressed to 43–48% that of the control (Fig. 3B). These results indicate that hnRNP A2/B1 is related to telomerase activity.

Analysis of heterogeneous nuclear ribonucleoprotein A2/B1 expression by immunohistochemistry

To characterize the clinicopathological significance of hnRNP A2/B1 expression in HCC, we performed immunohistochemical staining of hnRNP A2/B1 using paraffin-embedded tumor and non-tumor specimens from 74 HCC patients. We observed hnRNP A2/B1 expression in all HCC specimens, while it was expressed in 16 of 74 (22%) adjacent non-cancerous liver specimens ($P< 0.001$). We did not observe hnRNP A2/B1 expression in normal liver ($n = 5$) or in the early stage (F1–2) of chronic hepatitis ($n = 5$) (data not shown).

Interestingly, we noticed that anti-hnRNP A2/B1 antibody reacted to nuclear and cytoplasmic isoforms of hnRNP A2/B1. We defined HCC cells in which only nuclear hnRNP A2/B1 was expressed in tumor cells as nuclear hnRNP A2/B1-positive HCC (Fig. 4A). Similarly, both nuclear and cytoplasmic hnRNP A2/B1 was expressed in tumor cells as nuclear and cytoplasmic hnRNP A2/B1-positive HCC, respectively (Fig. 4B). Western blotting analysis showed that hnRNP A2/B1 was expressed significantly more, about 2.5-fold, in the nuclear and cytoplasmic hnRNP A2/B1-positive HCC than in the nuclear hnRNP A2/B1-positive HCC Fig. 5A, B).

The expression pattern of hnRNP A2/B1 in the nucleus and the cytoplasm was different in each HCC tissue type. Nuclear hnRNP A2/B1-positive HCC was observed in 40.5% (30 of 74) of HCC patients, whereas nuclear and cytoplasmic hnRNP A2/B1-positive HCC was observed in 59.5% (44 of 74) of HCC patents (Table 2). We then compared the clinicopathological features of nuclear hnRNP A2/B1-positive HCC and nuclear and cytoplasmic hnRNP A2/B1-positive HCC (Table 2). Nuclear and cytoplasmic expression of hnRNP A2/B1 was frequently observed in patients with a progressive histological grading (Edmondson-Steiner grades; $P = 0.002$) and microvascular invasion ($P = 0.013$) (Table 2). No relationship was apparent between the expression pattern of hnRNP A2/B1 and age, gender, type of infected virus, Child-Pugh score, AFP value, PIVKA-II value, tumor size, tumor morphology, TNM stages, or recurrence rate of HCC (Table 2). Importantly, survival analysis using the Kaplan-Meier method revealed that HCC patients with nuclear and cytoplasmic expression of hnRNP A2/B1 showed a significant lower survival rate than those with nuclear expression of hnRNP A2/B1 (log-rank test, $P = 0.0027$; Fig. 6). Furthermore, univariate Cox regression analysis showed that nuclear and cytoplasmic expression of hnRNP A2/B1 was significantly associated with low patient survival (HR, 2.37; 95% CI, 1.33–4.23;

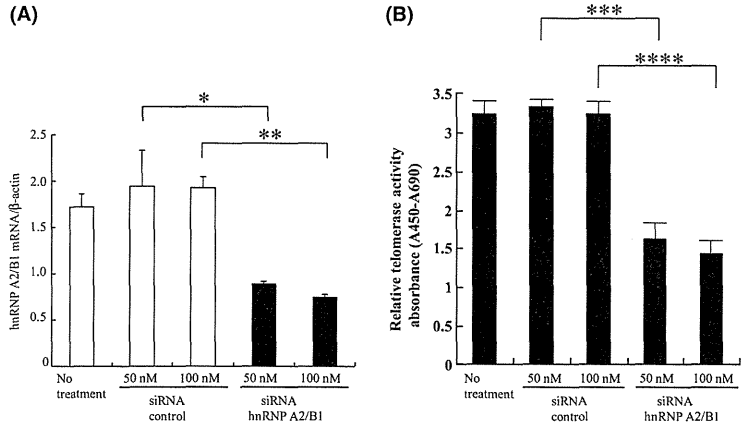

Fig. 3. siRNA against hnRNP A2/B1 suppresses telomerase activity. (A) mRNA expression of hnRNP A2/B1 after small interfering (si)RNA transfection in Huh7 cells transfected with sihnRNP A2/B1 and that of control siRNAs. Levels of mRNA were determined by real time polymerase chain reaction (PCR). (B) The activity of each lysate was determined by TRAP ELISA (*,**,***,****$P < 0.05$).

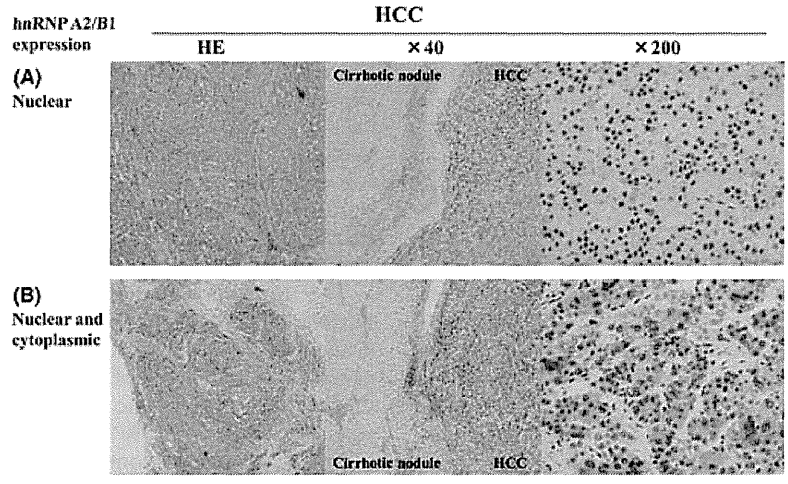

Fig. 4. Immunohistochemical analysis of hnRNP A2/B1 expression in HCC and adjacent cirrhotic liver tissue. A representative photomicrograph of hematoxylin and eosin staining and hnRNP A2/B1 staining in HCC tissue (× 40 and × 200, respectively) and adjacent cirrhotic liver tissue (× 40). (A) Nuclear hnRNP A2/B1-positive HCC. (B) Nuclear and cytoplasmic hnRNP A2/B1-positive HCC.

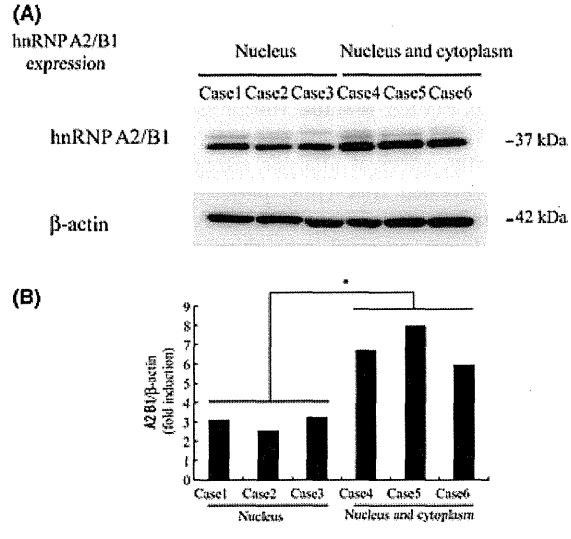

Fig. 5. The protein expression of hnRNP A1/B2 in HCC tissue. (A) Equal amounts of HCC tissue from Nuclear hnRNP A2/B1-positive HCC (cases 1–3) and Nuclear and cytoplasmic hnRNP A2/B1-positive HCC (cases 4–6) were loaded into the SDS-PAGE gel and normalized by comparing with β-actin. (B) The value in the graph is presented as mean ± SD (*$P < 0.05$).

$P = 0.004$) (Table 3). Multivariate Cox regression analysis showed that nuclear and cytoplasmic expression of hnRNP A2/B1 was an independent prognostic factor associated with low patient survival (HR, 3.86; 95% CI, 1.80–8.28; $P = 0.001$). Other clinicopathological features did not add independent prognostic information in this study (Table 3). These results demonstrate that

Table 2. Clinicopathological characteristics and hnRNP A2/B1 expression of nucleus (&) cytoplasm in HCC (n = 74)

hnRNP A2/B1 expression	nuclear (n=30)	nuclear and cytoplasm ic (n=44)	P-value
Age (<60 years/ ≥ 60 years)	12/18	18/26	0.938
Gender (male/female)	22/8	18/26	0.531
Virus (HBV/HCV/NBNC)	5/21/4	14/21/9	0.160
Child-Pugh (5/6/7)	28/2/0	37/5/2	0.377
AFP (<100 ng/ml/ ≥ 100 ng/ml	20/10	26/18	0.509
PIVKA-II (<100 mAU/ ml/ ≥ 100 mAU/ml	18/12	22/22	0.397
Histological grading (well/moderately/poorly)	12/18/0	0/32/12	0.002
Tumor size (<3 cm/ ≥ 3 cm)	16/14	22/22	0.778
Tumor morphology (uni/multi)	26/4	35/9	0.429
TMN classification (I/II/III/IVa)	6/17/6/1	2/27/10/5	0.139
Microvascular invasion (Yes/No)	11/19	29/15	0.013
HCC recurrence (Yes/No)	11/19	20/24	0.452

AFP, α-fetoprotein; HBV, Hepatitis B virus; HCC, hepatocellular carcinoma; HCV, Hepatitis C virus.

the expression of hnRNP A2/B1 correlates with the severity and progression of HCC and that nuclear and cytoplasmic hnRNP A2/B1 expression could be a useful biomarker for predicting the survival of HCC patients after surgical resection.

Discussion

The development of useful biomarkers for the early detection and prediction of HCC is urgently required to improve prognosis of patients with HCC. Moreover,

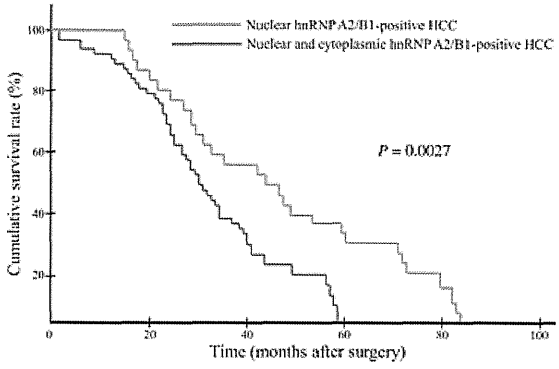

Fig. 6. Kaplan-Meier survival analysis of nuclear (and) cytoplasmic hnRNP A2/B1-positive HCC (log rank test).

biomarkers reflecting malignant features of HCC might be useful for the following patients and HCC therapy selection since HCC relapse frequently occurs in residual liver where HCC has been curatively removed by surgical treatment. Although AFP and PIVKA II are reliable tumor markers for the detection of recurrence of HCC, more than 50% of patients with small HCC (<2 cm) test negative for these markers(23).

A two-dimensional electrophoresis and mass spectrum-based proteomic strategy provide high-throughput simultaneous identification of hundreds of proteins; such a strategy is considered very valuable for screening tumor biomarkers(24, 25). Here, we applied a different approach for identifying telomerase-associated proteins in this study. According to previously reported methods (12), protein lysates of HCC tissue and non-cancerous tissue were subjected to HPLC gel filtration. A previous study using a soluble fraction of Huh7 cells identified two peak of endogenous hTERT at around 680 kDa and 350 kDa (data not shown). It was speculated that a dimer form of hTERT existed in the 680 kDa peak and a monomer in the 350 kDa peak. Hsp90 was exclusively distributed in the 350 kDa peak but not in the 680 kDa peak (data not shown). Unlike previous studies using Huh7 cells, we could not detect the 680 kDa peak fraction in HCC tissue. We could however detect the 350 kDa peak and the 200 kDa peak fraction in HCC tissue. The telomerase complex existed in the 350 kDa peak fraction. Moreover, Hsp90 existed in 350 kDa peak fraction, while many of the metabolic-related proteins were identified in the 200 kDa peak fraction. These data suggest that hTERT-associated proteins might exist in the 350 kDa peak fraction in HCC tissue.

Further analysis of the fractionated lysates of 350 kDa by LC-MS/MS revealed that 24 proteins were differentially expressed in HCC tissue when compared with nontumor tissue. In addition, 9 of the 24 proteins were already known as HCC-related proteins(14–20). We therefore focused on hnRNP A2/B1, one of the most abundant and important nuclear RNA-binding proteins involved in packaging nascent mRNA, alternative splicing(26, 27) and cytoplasmic RNA trafficking(28), translation(29), and stabilization(30).

To our knowledge, this is the first demonstration of hnRNP A2/B1 interaction with hTERT by immunoprecipitation *in vitro* and *in vivo*. hnRNP A2/B1 acts as a molecular adapter between single-stranded telomeric repeats or telomerase RNA (hTERC), and another segment of single-stranded DNA(31, 32). However the details for such an interaction need further investigation. Of the telomerase-related proteins, Hsp90 has been shown to be a functionally critical factor for telomerase activity *in vivo* and *in vitro*(33). The telomerase complex with Hsp90 within the 350 kDa complex was also detected in this study, confirming the biological functionality of telomerase activity (Fig. 1B,C). Hsp90 inhibitors reduce the amount of hTERT as well as telomerase activity(12). Despite the concentration of Hsp90

Table 3. Cox regression analysis of cumulative survival rate relative to nuclear and cytoplasmic hnRNP A2/B1 expression and clhicopathobgical parameters of primary HCC patients (*n*=74)

	Univariate		Mulivarate	
Variables	HR (95%CI)	*P*-value	HR (95%CI)	*P*-value
Age ≥ 60 years	1.25 (0.74–2.11)	0.453		
Male gender	1.16 (0.69–2.05)	0.606		
Child-Pugh ≥ 6	1.01 (0.36–2.84)	0.979		
AFP ≥ 100 ng/ml	1.42 (0.84–2.41)	0.188	1.25 (0.72–2.18)	0.429
PIVKA-II ≥ 100 mAU/ml	1.44 (0.85–2.45)	0.171	1.05 (0.59–1.90)	0.864
Histological grade (poorly)	1.33 (0.60–2.96)	0.485		
Tumorisize ≥ 3 cm	1.37 (0.83–2.25)	0.225		
Tumor morphology (multi)	1.09 (0.57–2.06)	0.797		
TMN cfessificaton (III, IVa)	1.63 (0.89–2.96)	0.112	1.24 (0.65–2.36)	0.51
Microvascular invasion (Yes)	1.08 (0.65–1.79)	0.765		
HCC recurrence (Yes)	0.73 (0.44–1.23)	0.238		
Nuclear and cytoplasmic hnRNP A2/B1	2.37 (1.33–4.23)	0.004	2.18 (1.19–4.00)	0.012

AFP, α-fetoprotein; HCC, hepatocellular carcinoma.

inhibitors, no telomere shortening of Hsp90 inhibitor-treated cells was observed (data not shown). The present study also demonstrated that the suppression of hnRNP A2/B1 by siRNA inhibited telomerase activity *in vitro*. However, unlike Hsp90, the suppression of hnRNP A2/B1 could potentially shorten telomere length and inhibit cell proliferation, although such an hypothesis should be confirmed by further experiments.

To further examine the clinicopathological significance of hnRNP A2/B1, immunohistochemical staining in clinical HCC samples was performed. Both nuclear and cytoplasmic expression of hnRNP A2/B1 in HCC was significantly related to tumor differentiation and microvascular invasion of HCC (Table 2). Furthermore survival analysis showed a significant correlation between the high nuclear and cytoplasmic expression of hnRNP A2/B1 in HCC and the low survival rate of patients (Table 3, Fig. 6). Although high nuclear and cytoplasmic expression of hnRNP A2/B1 in HCC was not associated with the recurrence rate of HCC (Tables 2, 3), it was associated with the recurrence pattern of HCC. Tumor morphology (multiple HCCs; $P = 0.100$) and vascular invasion ($P = 0.070$) in recurrence was observed more frequently in patients with nuclear and cytoplasmic hnRNP A2/B1-positive HCC than in those with nuclear hnRNP A2/B1-positive HCC, although the difference was not statistically significant (data not shown). The metastatic and invasive features of HCC with nuclear and cytoplasmic expression of hnRNP A2/B1 may contribute to the poor prognosis of affected patients.

Because hnRNP A2/B1 is a RNA shuttling factor(34), nuclear and cytoplasmic expression patterns might reflect increased hnRNP A2/B1 in cells; however, the expression of hTERT is presumably increased and colocalized with hnRNP A2/B1. It was reported that nucleolin, a molecule shuttling into and out of the nucleus, mediates hTERT and localization of hTERT shifted from the nucleus to the cytoplasm depending on its sublocalization(35). Increased hTERT might be associated with tumor differentiation, microvascular invasion and survival of HCC.

While preparing this study, Cui H. *et al.*(36) reported similar findings. They showed increased localization of hnRNP A2/B1 in the cytoplasm of HCC cells during dedifferentiation of HCC. Our study, however, showed the functional relevance of hnRNP A2/B1 on telomerase activity and demonstrated the clinical importance of hnRNP A2/B1 for patient survival.

In conclusion, employing a proteomic screening and molecular biology verification approach revealed a potential HCC biomarker, hnRNP A2/B1, and confirmed its usefulness in the diagnosis of and prediction of prognosis of HCC. Although the present data suggest that hnRNP A2/B1 is clinically significant, the understanding of its underlying mechanisms falls short of that required for the development of practical applications. Further approaches are thus needed to improve the diagnostic performance of hnRNP A2/B1 for biological and clinical detection of HCC.

Acknowledgements

We thank M. Baba, N. Nishiyama, and Y. Fujita for their technical assistance, and Drs. Y Hinoue, S Aoyama, and K Minouchi at Toyama City Hospital for their help with clinical support.

References

1. Thorgeirsson SS, Grisham JW. Molecular pathogenesis of human hepatocellular carcinoma. *Nat Genet* 2002; **31**: 339–46.
2. Parkin DM, Bray F, Ferlay J, Pisani P. Global cancer statistics. *CA Cancer J Clin* 2005; **55**: 74–108.
3. de Lange T. Ending up with right partner. *Nature* 1998; **392**: 753–54.
4. Blackburn EH. Telomere states and cell fates. *Nature* 2000; **408**: 53–6.
5. Bodnar AG, Ouellette M, Frolkis M, *et al.* Extension of life-span by introduction of telomerase into normal human cells. *Science* 1998; **279**: 349–52.
6. Feng J, Funk WD, Wang SS, *et al.* The RNA component of human telomerase. *Science* 1995; **269**: 1236–41.
7. Weinrich SL, Pruzan R, Ma L, *et al.* Reconstitution of human telomerase with the template RNA component hTR and the catalytic protein subunit hTRT. *Nat Genet* 1997; **17**: 498–502.
8. de Lange T. Protection of mammalian telomerase. *Oncogene* 2002; **21**: 532–40.
9. Yan P, Benhattar J, Seelentag W, Stehle JC, Bosman FT. Immunohistochemical localization of hTERT protein in human tissues. *Histochem Cell Biol* 2004; **121**: 391–7.
10. Desmet VJ, Gerber M, Hoofnagle JH, Manns M, Scheuer PJ. Classification of chronic hepatitis: diagnosis, grading and staging. *Hepatology* 1994; **19**: 1513–20.
11. Shirota Y, Kaneko S, Honda M, Kawai FH, Kobayashi K. Identification of differntially expressed genes in hepatocellular carcinoma with cDNA microarrays. *Hepatology* 2001; **33**: 832–40.
12. Mizuno H, Khurts S, Seki T, *et al.* Human telomerase exists in two distinct active complexes *In Vivo*. *J Biochem* 2007; **141**: 641–52.
13. Masutomi K, Yu EY, Khurts S, *et al.* Telomerase maintains telomere structure in normal human cells. *Cell* 2003; **114**: 241–53.
14. Kim SY, Lee PY, Shin HJ, *et al.* Proteomic analysis of liver tissue from HBx-transgenic mice at early stages of hepatocarcinogenesis. *Proteomic* 2009; **22**: 5056–66.
15. Sun W, Xing B, Sun Y, *et al.* Proteomic analysis of hepatocellular carcinoma by two-dimensional difference gel electrophoresis. *Mol Cell Proteomics* 2007; **6**: 1798–808.
16. Mohammad HS, Kurikihchi K, Yoneyama H, *et al.* Annexin A2 expression and phosphorylation are up-regulated in hepatocellular carcinoma. *Int J Oncol* 2008; **33**: 1157–63.
17. Liang CRM, Leow CK, Neo JCH, *et al.* Proteomic analysis of human hepatocellular carcinoma tissues by two-dimensional difference gel electrophoresis and mass spectrometry. *Proteomics* 2005; **5**: 2258–71.

18. Na K, Lee EY, Lee HJ, *et al.* Human plasma carboxylesterase 1, a novel serologic biomarker candidate for hepatocellular carcinoma. *Proteomics* 2009; **9**: 3989–99.
19. Goldenberg D, Ayesh S, Schneider T, *et al.* Analysis of differentially expressed gnes in hepatocellular carcinoma. *Mol Carcinog* 2002; **33**: 113–24.
20. Yokoyama Y, Kuramitsu Y, Takashima M, *et al.* Proteomic profiling of proteins decreased in hepatocellular carcinoma from patients infected with hepatitis C virus. *Proteomics* 2004; **4**: 2111–6.
21. Zhou J, Mulshine JL, Unsworth EJ, *et al.* Purification and characterization of a protein that permits early detection of lung cancer Identification of heterogeneous nuclear ribonucleoprotein-A2/B1 as the antigen for monoclonal antibody 703D4.. *J Biol Chem* 1996; **271**: 10760–6.
22. Jing GJ, Xu DH, Shi SL, *et al.* Aberrant expression and localization of hnRNP-A2/B1 is a common event in human gastric adenocarcinoma. *J Gastroenterol Hepatol* 2011; **26**: 108–15.
23. Marrero JA. Screening tests for hepatocellular carcinoma. *Clin Liver Dis* 2005; **9**: 235–51.
24. Celis JE, Gromov P. Proteomics in translational cancer research: toward an integrated approach. *Cancer Cell* 2003; **3**: 9–15.
25. Kawada N. Cancer serum proteomics in gastroenterology. *Gastroenterology* 2006; **130**: 1917–19.
26. Mayeda A, Munroe S, Caveres J, Krainer A. Function of conserved domains of hnRNP A1 and other hnRNP A/B proteins. *EMBO J* 1994; **13**: 5483–95.
27. Abdul-Manan N, Williams K. hnRNP A1 binds promiscuously to oligoribonucleotids: utilization of random and homo-oligonucleotides to discriminate sequence from base-specific binding. *Nucleic Acids Res* 1996; **24**: 4063–70.
28. Munro TP, Magee RJ, Kidd GJ, *et al.* Mutational analysis of a heterogeneous nuclear ribonucleoprotein A2 response element for RNA trafficking. *J Biol Chem* 1999; **274**: 34389–95.
29. Hamilton BJ, Nagy E, Malterg JS, Arrick BA, Rigby WFC. Association of heterogeneous nuclear ribonucleoprotein A1 and C proteins with reiterated AUUUA sequences. *J Biol Chem* 1993; **268**: 8881–7.
30. Hamilton BJ, Burns CM, Nichols RC, Rigby WFC. Modulation of AUUUA response element binding by heterogeneous nuclear ribonucleoprotein A1 in human T lymphocytes. *J Biol Chem* 1997; **274**: 34389–95.
31. Kim MJ, Lyndal W, Derek DK, *et al.* hnRNP A2, a potential ssDNA/RNA molecular adapter at the telomere. *Nuleic Acids Res* 2005; **33**: 486–96.
32. Kamma H, Fujimoto M, Fujiwara M, *et al.* Interaction of hnRNP A2/B1 isoforms with telomeric ssDNA and the *in Vitro* function. *Biochem Biophys Res Commun* 2001; **280**: 625–30.
33. Holt SE, Aisner DL, Baur J, *et al.* Functional requirement of p23 and Hsp90 in telomerase complexes. *Genes Dev* 1999; **13**: 817–26.
34. Nakielny S, Dreyfuss G. Nuclear export of proteins and RNAs. *Curr Opin Cell Biol* 1997; **9**: 420–29.
35. Khurts S, Masutomi K, Delgermaa L, *et al.* Nucleolin interacts with telomerase. *J Biol Chem* 2004; **279**: 51508–15.
36. Cui H, Wu F, Sun Y, Fan G, Wang Q. Up-regulation and subcellular localization of hnRNP A2/B1 in the development of hepatocellular carcinoma. *BMC cancer* 2010; **10**: 356–69.

OPEN ACCESS Freely available online

PLoS one

Novel Evidence of HBV Recombination in Family Cluster Infections in Western China

Bin Zhou[1], Zhanhui Wang[1], Jie Yang[1], Jian Sun[1], Hua Li[2], Yasuhito Tanaka[3], Masashi Mizokami[4], Jinlin Hou[1]*

1 Institute of Hepatology, Nanfang Hospital, Southern Medical University, Guangzhou, Guangdong, China, **2** Qinghai Provincial Infectious Diseases Hospital, Xining, Qinghai, China, **3** Department of Virology and Liver Unit, Nagoya City University Graduate School of Medical Sciences, Kawasumi, Mizuho, Nagoya, Japan, **4** The Research Center for Hepatitis and Immunology, National Center for Global Health and Medicine, Kounodai, Ichikawa, Japan

Abstract

Two hepatitis B virus (HBV) C/D recombinants were isolated from western China. No direct evidence indicates that these new viruses arose as a result of recombination between genotype C and D or a result of convergence. In this study, we search for evidence of intra-individual recombination in the family cluster cases with co-circulation of genotype C, D and C/D recombinants. We studied 68 individuals from 15 families with HBV infections in 2006, identified individuals with mixed HBV genotype co-infections by restriction fragment length polymorphism and proceeded with cloning and DNA sequencing. Recombination signals were detected by RDP3 software and confirmed by split phylogenetic trees. Families with mixed HBV genotype co-infections were resampled in 2007. Three of 15 families had individuals with different HBV genotype co-infections in 2006. One individual (Y2) had a triple infection of HBV genotype C, D and C/D recombinant in 2006, but only genotype D in 2007. Further clonal analysis of this patient indicated that the C/D recombinant was not identical to previously isolated CD1 or CD2, but many novel recombinants with C2, D1 and CD1 were simultaneously found. All parental strains could recombine with each other to form new recombinant in this patient. This indicates that the detectable mixed infection and recombination have a limited time window. Also, as the recombinant nature of HBV precludes the possibility of a simple phylogenetic taxonomy, a new standard may be required for classifying HBV sequences.

Citation: Zhou B, Wang Z, Yang J, Sun J, Li H, et al. (2012) Novel Evidence of HBV Recombination in Family Cluster Infections in Western China. PLoS ONE 7(6): e38241. doi:10.1371/journal.pone.0038241

Editor: Darren P. Martin, Institute of Infectious Disease and Molecular Medicine, South Africa

Received December 13, 2011; **Accepted** May 2, 2012; **Published** June 4, 2012

Funding: This work was supported by grants from National twelve-five project of China (2012ZX10002-004), National eleven-five project of China (2009ZX10004-314) and National Natural Science Foundation of China (Grant number: 30872245). The funders had no role in study design, data collection and analysis, decision to publish, or preparation of the manuscript.

Competing Interests: The authors have declared that no competing interests exist.

* E-mail: jlhousmu@yahoo.com.cn

Introduction

Not all viruses are equally prone to recombination. Recombination has not been detected in several viruses despite repeated searches [1]. Whether recombination does or does not exist is important for understanding the evolution and replication mechanism of a specific kind of virus. Hepatitis B virus (HBV), a major human pathogen, has been classified into 10 genotypes and several sub-genotypes [2,3]. Many sub-genotypes were identified by polygenetic analysis as recombinants. But there is no direct evidence to indicate that these subgenotypes arose as a result of recombination or perhaps a result of convergence.

Coinfection with different HBV genotype strains is a prerequisite for recombination. As more than one genotype is predominant in most of the geographic regions, coinfection between the predominating HBV genotypes is not a rare finding, especially for B and C, or A and D. The prevalence of mixed HBV genotype infections has been reported using varied genotyping methods [4,5,6].

Our previous study found two kinds of HBV C/D recombinants in northwest China [7]. In a further study of ethnic groups of five provinces, we confirmed the geographic and ethnic distribution of the HBV C/D recombinant in northwest China [8], and found that family-cluster HBV infections were common in these endemic areas. We hypothesize that infected members of HBV family clusters would gain exposure to various genotypes through marriage, while at the same time; competent strains would be selected through vertical transmission. It would be useful to observe the mixed infection in family-cluster cases, especially in patients infected with C/D recombinants.

The aim of this study was to evaluate the possibility of recombination between two HBV genotypes within an individual by finding cluster-infected families in which individual members were infected with different HBV genotypes. We would then look for individuals within these families with multiple-genotypes that were likely to have been obtained from other family members as a result of vertical or horizontal transmission. Novel viral genomes within an individual with a multiple genotype infection that were mosaics of the known viral genotypes in the family, but not present in any of the other family members, would be consistent with the hypothesis that they arose within the individual with multiple genotype infections.

Methods

Subjects

We enrolled 68 patients with a chronic HBV infection from 15 families. All the families were from a district located at the boundary of Gansu and Qinghai provinces, where the prevalence of genotype C2, D1 and C/D recombinant HBV were known to be high [8]. The families were initially identified with cluster HBV infection in an epidemiological survey in 2002. Sixty-eight individuals were sampled in June 2006 and December 2007 for the purpose of assigning HBV genotypes to chronically infected individuals and finding individuals with multiple HBV genotype co-infections. None of the patients received anti-viral therapy or immunosuppressant drugs. A written, informed consent was obtained from each family, and the study protocol was approved by the Southern Medical University Ethics Committee.

HBV DNA Extraction and HBV Genotyping

HBV DNA was extracted from 400 μL of serum by QIAamp UltraSens Virus Kit (Qiagen GmbH, Germany), then re-suspended in 50 μL water and stored at −20°C until analysis. HBV genotypes, including C/D recombinant, were initially assigned using the PCR based restriction fragment length polymorphism (RFLP) methods described previously [9], [8].

Cloning of Mixed Infection Samples

For samples with mixed genotype infections, PCR cover HBV S gene (nt136-1110) was performed using the primers and thermocycling conditions descirbed by Sugauchi et al [10]. For samples needing further recombination analysis, PCR was performed using the primers and thermocycling conditions described by Günther to obtain full-length HBV genome [11]. Alternatively, a nested PCR was used to produce two overlapping fragments in subjects with low HBV DNA levels as described by Sugauchi et al [12]. The spanning of fragment A cover nucleotides 2813 to 1824, and fragment B included nucleotides 1821 to 237. LA-Taq (TAKARA, Japan) and high-fidelity polymerase COD-FX (TOYOBO, Japan) were used to produce amplimers for cloning and direct sequencing respectively. Finally, Fragment C (HBV nt56-nt1824) was obtained from a PCR amplification of Y2 HBV-DNA to which an aliquot of genotype B HBV-DNA had been added. The purpose of this experiment with in-tube control of genotype B was to determine if the recombinant clones were being generated during the PCR amplification. PCR products were gel-purified and cloned into the PMD19-T vector (TAKARA, Japan) according to the manufacturer's instructions, and used to transform JM109 competent cells (TAKARA, Japan). A minimum of 15 clones were sequenced from subjects with a mixed-strain infection and three clones were sequenced from family members with a single-strain infection. All sequencing of clones and PCR products was performed by Invitrogen Ltd. (Shanghai, China).

Phylogenetic and Recombination Analysis

Genotypes of clones were determined by phylogenetic tree analysis and recombination analysis. The sequences were assembled using SeqMan II software (DNAStar Inc.). Sequence alignments were performed using ClustalW and confirmed by visual inspection. Phylogenetic trees were constructed by the neighbour-joining (NJ) method (Saitou & Nei, 1987). To confirm the reliability of the phylogenetic tree analysis, bootstrap resampling and reconstruction were carried out 1000 times. A phylogenetic tree analysis of HBV strains isolated from the mixed infection family was compared with reference strains from GenBank. Accession numbers are indicated on the tree. Bootstrap values are shown along each main branch. The lengths of the horizontal bars indicate the number of nucleotide substitutions per site. The regions included in the analysis were the same with fragment A, B and C or a little shorter. Phylogenetic and molecular evolutionary analyses were conducted using MEGA version 5 (Tamura, Peterson, Stecher, Nei, and Kumar 2011).

Recombination signals were initially detected by RDP3.β.4 software [13,14]. Bootscan, Geneconv and Siscan were used. The highest acceptable P-value was 0.05. Bootscan and Siscan window sizes were 300 bp, step size was 30, replicates for 100 times. A genotype F sequence (GenBank accession numbers is X75658 and X75663) was used as external reference. The precise map of recombination was determined by split phylogenetic tree and alignment. Split phylogenetic trees were constructed by the method same as above. In alignment, each clone was compared to reference C2, D1 and CD1 consensus sequences. We then inspected the alignments to determine the identical crossover sequences around the breakpoint within which the recombination occurred.

Accession Number of the Sequences

GenBank accession number of reference sequences of HBV genotype C2, D1, CD1 and CD2 are indicated in phylogenetic tree. Accession Numbers of Y2 clones are JX036326-JX036359.

Results

Mixed-genotype Infections in HBV Cluster Families

Different HBV genotypes were found in three families among 15 families. The flow of participants in the study and family trees of families with mixed genotypes/subgenotypes of HBV infection are shown (Figure 1).

Family V had infected members across two generations and two genotypes: In 2006, the mother (V1W) and daughter (V2F) were infected with subgenotype D1 while the son (V2M) had a CD1 recombinant. In 2007, the daughter (V2F) had subgenotype D1 while other family members had HBV DNA levels below the detection limit of the nested PCR assay.

Family Q had infected members across three generations and two genotypes/subgenotypes. In 2006, the grandmother (Q1W) and grandson (Q3M) were infected with CD1 recombinant while father (Q2) and granddaughter (Q3F) had mixed infections of genotype C2 and CD1 recombinants. In 2007, the same genotypes were detected in all family members except that the granddaughter (Q3F) had an HBV DNA level below the detection limit of the nested PCR assay.

Family Y had affected members across three generations and three genotypes/subgenotypes. In 2006, the grandfather of family Y (Y1) was infected with genotype C2 while grandmother (Y1W) had mixed infections of CD1 and C2. Mother (Y2W) and granddaughter (Y3F) were infected with the CD1 recombinant. Father (Y2) had triplicate infections of genotype C2, D1 and CD recombinant. Grandson's (Y3M) serum was unavailable. In 2007, the grandfather (Y1) and mother (Y2W) had HBV DNA levels below the detection limit while the grandmother (Y1W) and granddaughter (Y3F) had genotype CD1. Father (Y2) and grandson (Y3M) had genotype D1.

Phylogenetic Analysis of Family Y, Family Q and Family V

A phylogenetic tree constructed from HBV nt 36-1110 from the clones of family Y is given (Figure 2A). The clones (dotted) of family Y exhibits three clusters on genotype C2, D1 and CD1.

The phylogenetic tree construct from HBV nt136-1110 from the clones of families Q and V is given (Figure 2B). The clones of

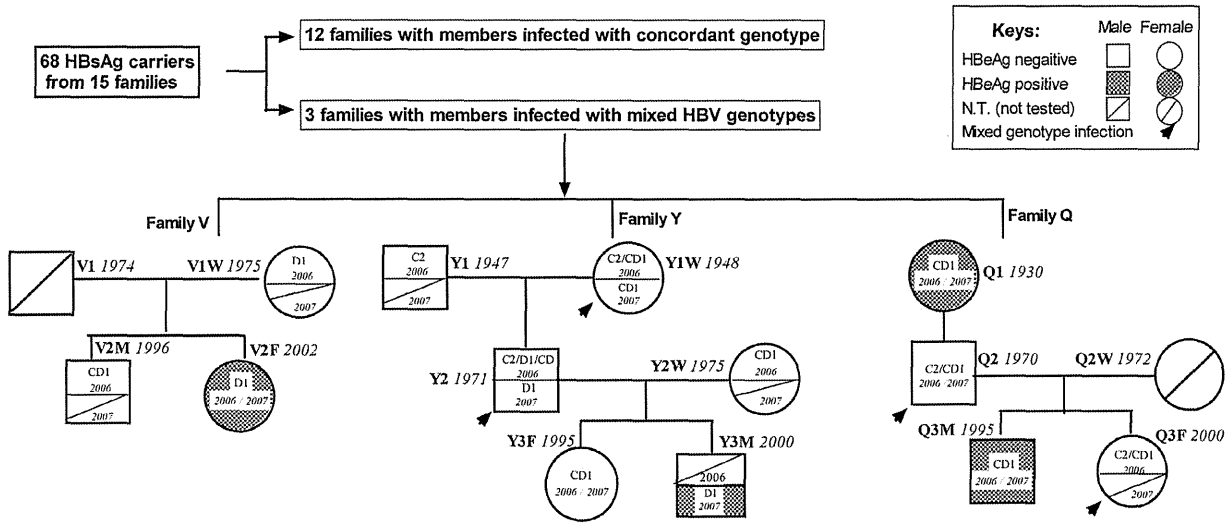

Figure 1. Flow of participants in the study and family trees of family with mixed genotypes/subgenotypes HBV infection. Circles and rectangles correspond to female and male individuals, respectively. Family name and birth date of the patients are indicated beside the circles and rectangles. Subgenotype and the year of blood sampling are indicated inside the circles and rectangles. Family V with affected members across two generations and two genotypes/subgenotypes. Family Q with affected members across three generations and two genotypes/subgenotypes. Family Y with affected members across three generations and three genotypes/subgenotypes. Specially, father (Y2) of family Y with triplicate infection of genotype C, D and CD recombinant in 2006. N.T: Not tested for HBV DNA level below the detection limit of the nested PCR assay or no serum was available.
doi:10.1371/journal.pone.0038241.g001

family Q (indicated by black dots) exhibit two clusters of subgenotypes C2, and CD1. The clones (indicated by black triangles) from family V exhibit two clusters of subgenotypes D1 and CD1.

A phylogenetic tree constructed from HBV nt 36-1110 of novel recombinants clones of Y2 is given in Figure 2C. The dotted clones are from Y2. The topology of phylogenetic tree with recombinants is totally different from typical trees. Recombinant sequences blurred the typical branch,in other words, blurred the typical genotype.

Recombination and Crossover Analysis of Quasi-species of Y2

Results of recombination analysis of Y2 clones are as bellow: Three kinds of analytical methods certificated the same recombination map. The initial pictures of the three methods were all provided as supplemental figures. Recombination events detected by RDP software are shown in Figure S1, S2, and S3. Split phylogenetic trees constructed by MEGA software are shown in Figure S4, S5, and S6, (clone number and fragment used to construct tree are indicated beside each tree). Sequence alignments are shown in Figure S7, S8, and S9.

The region where recombination breakpoints had the highest probabilities was recognized as crossover region, which is a region that one parental genotype switches to another. Upstream sequence of crossover region will have specific mutation of one genotype but with no specific mutation of another, downstream just opposite. At the same time, these two genotypes should share same sequence at crossover region. We indicated the crossover region in direct alignment by black bars in Figure S3 initially and marked it in recombination map by colorful bars in Figure 3A and black bars in Figure 3B. The clonal sequences of 2006 showed 17 unique crossover regions in fragments A, B and C. We could not identify any common motif within these sequences that might suggest a common mechanism for crossovers in the HBV. The size of switch region share the same sequence are different in different strains, from 6–174 bp (6 bp for Y2M-2 clone in Figure S7 and 174 bp for Y2M-29 clone in Figure S8).

To illustrate the recombination map in a simple way. An abbreviated alignment of fragment A, B and C are shown in Figure 3B. Green and pink bars indicated the genotype C2 and D1 respectively. Black bars showed the crossover region. The aligned sequences provide a snapshot of the recombinant HBV strains. Genotype C2, D1 and CD1 recombinant clones of Y2 were all used as parental sequences to recombine with each other to form new recombinants. A series of novel recombinants were found in three fragments.

In 15 clones of fragment A, there were five genotype C (Y2-6,9,13,14,15,); two genotype D (Y2-11,12); one CD1 (Y2-10) and seven novel different C/D recombination (Y2-1,2,4,7,8,3,5).

In 16 clones of fragment B, there were four genotype C (Y2-23,71,78,75); seven genotype D (Y2-25, 27,79,76,72,22,210); one CD1 (Y2-29) and four novel C/D recombinants (Y2-212,21 73,77).

Of the 56 clones of fragment C(in which genotype B HBVDNA were added as an in-tube control to exclude the recombination by PCR procedure), there were 32 pure genotype B clones; nine genotype C clones(Y2-B10,B5,B8,B9,B13,B16.B17.B18,B24); five genotype D clones(Y2-B22,B3,B4,B21,B23), two CD1 clones (Y2-B1,B11) and eight novel C/D recombinants (Y2-B6,B7,B14,B15,B19,B2,B12,B20). No recombinants of genotype B were found.

Discussion

Recombination is one of the major mechanisms contributing to the evolution of retroviruses [15]. Since the HBV has a reverse transcription step in its life cycle, it is conceivable that recombination also contributes to diversity in HBV genomes. Although just four cases were observed with mixed genotype

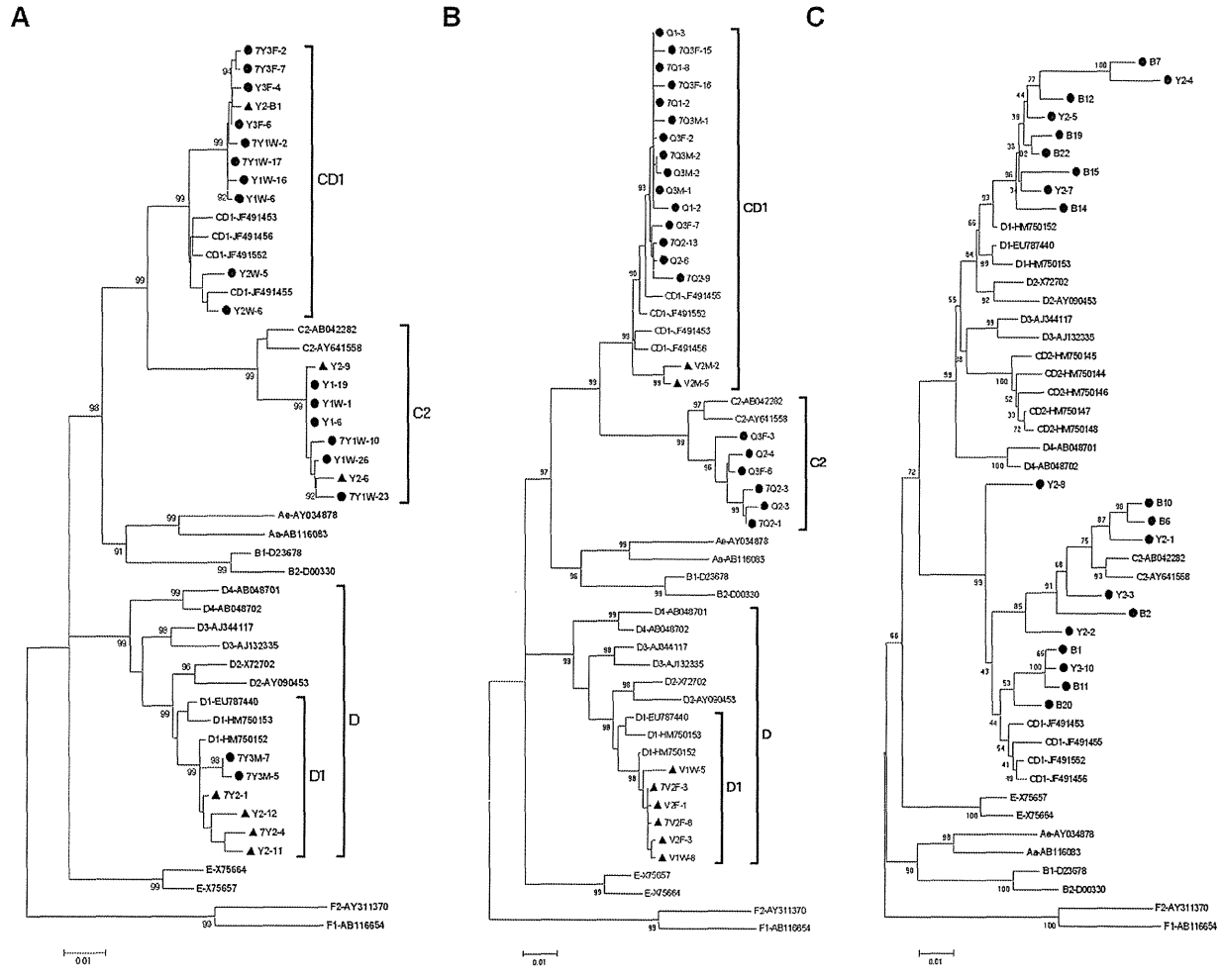

Figure 2. Phylogenetic tree construct by HBV nt 136-1110. (**A**) clones of family Y. Solid dots indicate the clones from Y1,Y1W,Y2W,Y3F and Y3M; Solid triangles indicate the clones from Y2. Family names starting with number 7 means the samples collected in 2007 otherwise in 2006. Novel recombinants of Y2 were excluded from the phylogenetic tree. (**B**) clones of family Q and family V. Solid dots indicate the clones from family Q; Solid triangles indicate the clones from family V. A family name starting with number 7 means the samples collected in 2007, otherwise, in 2006. (**C**) Novel recombinant clones of Y2. Solid dots indicate the clones from Y2.
doi:10.1371/journal.pone.0038241.g002

infections, we obtained a snapshot of naturally occurring HBV recombinants generated in the absence of selection and after selection. Our result showed direct evidence of HBV recombination, with new information of recombining crossovers compared with similar studies [16,17,18,19].

The recombination analysis of Y2 quasi-species showed variable types of recombinant between genotype C2, D1 and CD1 in 2006. Some studies show that hotspots of recombination most on the boundary of ORFs [12,20]. Our results showed that two or more strains of HBV can recombine with each other at any region along the genome. Crossover regions can be hundreds or just several base pairs, The length of crossover region is depends on the location of it on HBV genome. If it is located in a conserved HBV region, for another word, where many different genotypes share the same sequence, the length of crossover region may be long. If it is located in a non-conserved region, it may be very short. At the same time, we found that the crossover region distributed totally at random on HBV genome. Consistent with our results, *in vitro* evidence showed the initial recombination events in a laboratory system of MHV were almost entirely randomly distributed along the sequence [21]. It was only after passage through cell culture, with the opportunity for selection to remove less fit variants, that crossover sites became "localized" to just a small area of the region examined. Crucially, they also suggested initial products of recombination may go undetected because of the action of strong purifying selection which will remove new, deleterious combinations of mutations. The conclusion is therefore an interpretation for the genotype change of Y2. The Y2 presented multiple strain infections of C2/D1/CD1 and many new recombinants with no obvious dominant genotype strain in 2006. After 18 months, however, all the type C2 and CD recombinant strains disappeared while the D strain became dominant. A similar case of mixed HBV genotype infection in which one genotype was lost and another prevailed was previously described in patients with HBeAg seroconversion [4,22].

Epidemiologically, HBV genotype CD1 and C2 are the most common strains in ethnic minorities of northwest China with CD2 and D1 as minor strains. Precise mapping of recombination

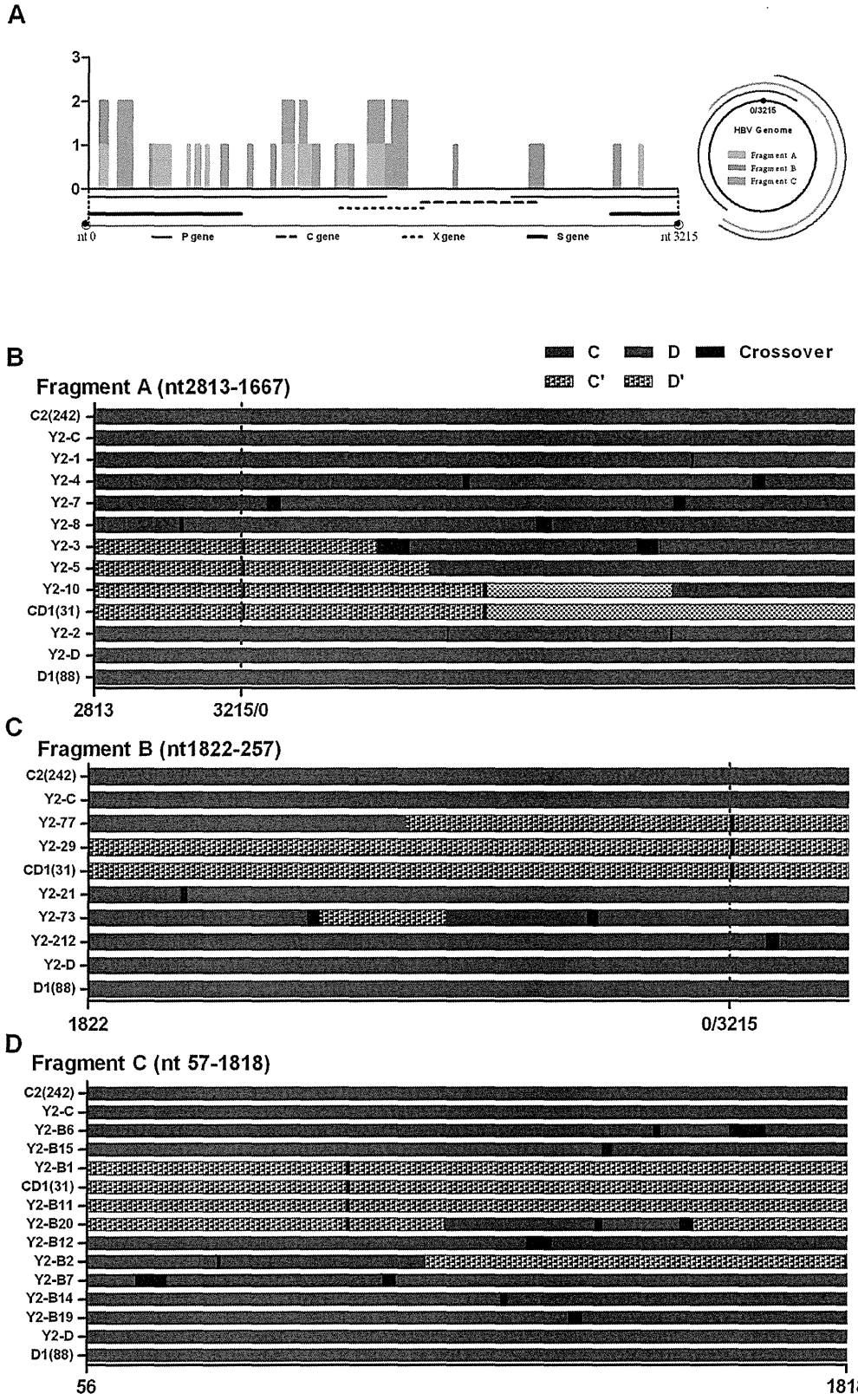
A
3
2
1
0
nt 0
P gene
C gene
X gene
S gene
nt 3215
0/3215
HBV Genome
Fragment A
Fragment B
Fragment C
B
C
D
Crossover
C'
D'
Fragment A (nt2813-1667)
C2(242)
Y2-C
Y2-1
Y2-4
Y2-7
Y2-8
Y2-3
Y2-5
Y2-10
CD1(31)
Y2-2
Y2-D
D1(88)
2813
3215/0
Fragment B (nt1822-257)
C2(242)
Y2-C
Y2-77
Y2-29
CD1(31)
Y2-21
Y2-73
Y2-212
Y2-D
D1(88)
1822
0/3215
Fragment C (nt 57-1818)
C2(242)
Y2-C
Y2-B6
Y2-B15
Y2-B1
CD1(31)
Y2-B11
Y2-B20
Y2-B12
Y2-B2
Y2-B7
Y2-B14
Y2-B19
Y2-D
D1(88)
56
1818

Figure 3. Alignment and recombination crossover regions found in Y2 clones. (**A**) Frequency and distribution of the recombination crossover regions found in Y2 clones along the HBV genome. The bars indicate the number of clones (y axis) showing recombination crossover regions at each site. The 1-3215 of x axis was consistent with the nt1-3215 of HBV genome. Different colors represent the sites find from clones of different PCR region: pink bars for fragment A, grey bars for fragment B and green bars for fragment C. (**B**) Alignment of fragment A (HBV nt 2813-0-1667). Y2-1'12: clones from fragment A of Y2 patients. (**C**) Alignment of fragment B (HBV nt 1822-0-257). Y2-21'212: clones from fragment B of Y2 patients. (**D**) Alignment of fragment C (HBV nt 57-1818) of Y2 clones. Y2-B1'B22: clones from fragment C of Y2 patients. The number on the x axis was consistent with the site of nucleotides of HBV genome. Solid green lines are genotype C2, solid pink lines are genotype D1, speckled green lines are the C2 component of genotype recombinant CD1 and speckled pink lines are the D1 component of recombinant genotype CD1. The black lines are sequence that is common to the recombining genotypes, and within which the recombination probably occurred. C2 (242) is the consensus sequence formed by 242 subgenotype C2 sequences from GenBank. D1 (88) is the consensus sequence formed by 88 subgenotype D1 sequences from GenBank. CD1 (33) is the consensus sequence formed by CD1 recombinant sequences from GenBank.
doi:10.1371/journal.pone.0038241.g003

suggests C2 and D1 are parental sequences of CD1 and CD2 recombinants. Virological differences among HBV genotypes were demonstrated in vitroand in CHiM mice, with genotype C having a higher replication capacity than D [23]. Why does the replication-deficient genotype D virus predominate over replication-competent genotype C? As mixed HBV infections together with recombination are rare, we have little knowledge about i this situation. On the one hand, we know little about host impact on different genotypes and recombinants. On the other hand, we know little about interference and competition in the quasi-species of mixed infection. In vitro results showed the replication capacity of individual clone, exclude the influence of host and other strains of quasi-species. An example from a ChiM mice study showed that monoinfection of HBV/G in ChiM mice display a very slow replication while coinfection with HBV/A remarkably enhanced the replication of HBV/G. The replication of HBV/G is heavily dependent on coinfection with other genotypes. When HBV/G superinfected on other genotypes, a rapidly takes over of HBV/G from original genotype were observed, though they are indispensable [24]. This study confirms that in a mixed infection system of different genotypes, the replication capacity of a genotype may be different from that of monoinfection. At the same time, replication capacity is not the only factor to influence which strain will become dominant. Variable recombinants found in our study may be mechanistically capable of genetic exchange, but strong selection guaranteed the elimination of hybrid genomes. The mechanism of selection in mixed infection also needs more investigation.

We found mixed HBV genotypes infection with many novel recombinants at one point in time, but just one genotype was found 18 months later. This may indicate that the detectable mixed infection and recombination has a limited time window due to the sensitivity of detection or strong selection power of the host. That's why in most studies, we can identify a major genotype in one patient. Even so, evolutionarily visible and invisible recombination of HBV could occur and play an important role by generating genetic variation or reducing mutational load. However, this study had limitation, because recombination signals were detected by RDP3 software and confirmed by split phylogenetic tree and alignment, indicating the recombinant or recombinant-like form should depend on the software. If we use another software, the results might be different.

Studies of HBV in endemic areas throughout the world have resulted in large numbers of full genome sequences available for phylogenetic analysis enabling the identification of novel, mosaic HBV genomes that appear to be the result of recombination between previously known sequences [7,25,26]. One of the most comprehensive analyses of putative HBV inter-genotype recombinants showed the existence of 24 phylogenetically independent HBV genomes involving all known human genotypes [27]. Some of these recombinants are unique to individual subjects, but some undergo expansion in specific populations and become recognized as new genotypes or subgenotypes [12,28,29,30]. Four stages in the process of generating popular HBV recombinant genomes should be recognized. The first stage is the co-circulation of different HBV strains or genotypes in the same geographic area. The second is the existence of individuals who have been infected with more than one strain of HBV. The third is the generation of a novel recombinant strain(s) within an individual. The fourth is the selection of a recombined strain with the ability to replicate and be transmitted. Our data show the natural process of the formation and selection of recombination though the recombinant strains of Y2 that appeared in 2006 that were all removed from samples in 2007.

By using phylogenetic trees and homology calculations, HBV variants infecting humans are currently classified into ten genotypes that differ from each other in nucleotide sequence by 7.5 to 13% [2,3]. There are some characteristic length differences between the genotypes that facilitates their detection and discrimination. However, as shown in Figure 2, existence of a recombinant makes the topology of the phylogenetic tree totally different from one with no recombinant. Recombinant strains obscured the definition of genotypes. Based on the algorithm creating a phylogenetic tree, sequences with high homologues cluster together. With the same logic, recombinants always clustered with the backbone parental sequence, in other words, with which they have high similarity with the larger proportion of the recombination region. Therefore, recombinants always seem to be a subgenotype of their backbone parental sequence. Similar to Y2-8 clone in Figure 2C, for recombinants with similar proportion of both parental genotypes, the sequence shows a divergent trend different from both parental genotypes.

Based on phylogenetic topology changes of different regions of HBV, it was hypothesized that some of the genotypes that are conventionally regarded as "pure," actually were recombinant. Genotype E strains show evidence of recombination with genotype D at 1950–2500. new reported genotype "I" actually belongs to genotype C. Furthermore, Subgenotype Ba possesses the recombination with genotype C at 1740 to 2485 [31,32,33]. Recombinants comprising regions with different histories have important implications for the way we think about HBV evolution. It means that there is no single phylogenetic tree that can describe the evolutionary relationships between genotypes.

In conclusion, mixed HBV genotypes infection with many novel recombinants at one point in time ended up with just one genotype 18 months later in this study. This may indicate that the detectable mixed infection and recombination have a limited time window due to the sensitivity of detection or strong selection power of the host. Also, as the recombinant or recombinant-like nature of HBV precludes the possibility of a "true" phylogenetic taxonomy, a new standard may be required for classifying HBV sequences.

Supporting Information

Figure S1 Recombination map of fragment A created by RDP software.
(TIF)

Figure S2 Recombination map of fragment B created by RDP software.
(TIF)

Figure S3 Recombination map of fragment C created by RDP software.
(TIF)

Figure S4 Split phylogenetic trees constructed by MEGA software. clone number and fragment used to construct trees are indicated beside each tree.
(TIF)

Figure S5 Split phylogenetic trees constructed by MEGA software. clone number and fragment used to construct trees are indicated beside each tree.
(TIF)

Figure S6 Split phylogenetic trees constructed by MEGA software. clone number and fragment used to construct trees are indicated beside each tree.
(TIF)

Figure S7 Alignment of fragment A(HBV nt 2813-0-1667)of Y2 clones. Deep green lines are genotype C2, deep pink lines are genotype D1, light green lines are the C2 component of genotype recombinant CD1 and light pink lines are the D1 component of recombinant genotype CD1. The black lines are sequence that is common to the recombining genotypes, and within which the recombination probably occurred. C2 (242): consensus sequence formed by 242 subgenotype C2 sequences from GenBank. D1 (88): consensus sequence formed by 88 subgenotype D1 sequences from GenBank. CD1 (33): consensus sequence formed by CD1 recombinant sequences from GenBank. Y2-1'12: clones from fragment A of Y2 patients.
(DOC)

Figure S8 Alignment of fragment B(HBV nt 1822-0-257) of Y2 clones. Deep green lines are genotype C2, deep pink lines are genotype D1, light green lines are the C2 component of genotype recombinant CD1, light pink lines are the D1 component of recombinant genotype CD1. The black lines are sequence that is common to the recombining genotypes, and within which the recombination probably occurred. C2 (242): consensus sequence formed by 242 subgenotype C2 sequences from GenBank. D1 (88): consensus sequence formed by 88 subgenotype D1 sequences from GenBank. CD1 (33): consensus sequence formed by CD1 recombinant sequences from GenBank. Y2-21'212: clones from fragment B of Y2 patients.
(DOC)

Figure S9 Alignment of fragment C(HBV nt 57-1818) of Y2 clones. Deep green lines are genotype C2, deep pink lines are genotype D1, light green lines are the C2 component of genotype recombinant CD1, light pink lines are the D1 component of recombinant genotype CD1. The black lines are sequence that is common to the recombining genotypes, and within which the recombination probably occurred. C2 (242): consensus sequence formed by 242 subgenotype C2 sequences from GenBank. D1 (88): consensus sequence formed by 88 subgenotype D1 sequences from GenBank. CD1 (33): consensus sequence formed by CD1 recombinant sequences from GenBank. BÌB22: clones from fragment C of Y2 patients.
(DOC)

Author Contributions

Conceived and designed the experiments: ZW MM JH. Performed the experiments: BZ ZW. Analyzed the data: BZ JY JS. Contributed reagents/materials/analysis tools: HL YT. Wrote the paper: BZ YT.

References

1. Bilsel PA, Rowe JE, Fitch WM, Nichol ST (1990) Phosphoprotein and nucleocapsid protein evolution of vesicular stomatitis virus New Jersey. J Virol 64: 2498–2504.
2. Okamoto H, Tsuda F, Sakugawa H, Sastrosoewignjo RI, Imai M, et al. (1988) Typing hepatitis B virus by homology in nucleotide sequence: comparison of surface antigen subtypes. J Gen Virol 69 (Pt 10): 2575–2583.
3. Norder H, Hammas B, Lofdahl S, Courouce AM, Magnius LO (1992) Comparison of the amino acid sequences of nine different serotypes of hepatitis B surface antigen and genomic classification of the corresponding hepatitis B virus strains. J Gen Virol 73 (Pt 5): 1201–1208.
4. Gerner PR, Friedt M, Oettinger R, Lausch E, Wirth S (1998) The hepatitis B virus seroconversion to anti-HBe is frequently associated with HBV genotype changes and selection of preS2-defective particles in chronically infected children. Virology 245: 163–172.
5. Liu CJ, Kao JH, Chen DS (2006) Mixed hepatitis B virus genotype infections: the more, the worse? Hepatology 44: 770.
6. Lin CL, Liu CJ, Chen PJ, Lai MY, Chen DS, et al. (2007) High prevalence of occult hepatitis B virus infection in Taiwanese intravenous drug users. J Med Virol 79: 1674–1678.
7. Wang Z, Liu Z, Zeng G, Wen S, Qi Y, et al. (2005) A new intertype recombinant between genotypes C and D of hepatitis B virus identified in China. J Gen Virol 86: 985–990.
8. Zhou B, Xiao L, Wang Z, Chang ET, Chen J, et al. (2011) Geographical and ethnic distribution of the HBV C/D recombinant on the Qinghai-Tibet Plateau. PLoS One 6: e18708.
9. Zeng GB, Wen SJ, Wang ZH, Yan L, Sun J, et al. (2004) A novel hepatitis B virus genotyping system by using restriction fragment length polymorphism patterns of S gene amplicons. World J Gastroenterol 10: 3132–3136.
10. Sugauchi F, Mizokami M, Orito E, Ohno T, Kato H, et al. (2001) A novel variant genotype C of hepatitis B virus identified in isolates from Australian Aborigines: complete genome sequence and phylogenetic relatedness. J Gen Virol 82: 883–892.
11. Gunther S, Li BC, Miska S, Kruger DH, Meisel H, et al. (1995) A novel method for efficient amplification of whole hepatitis B virus genomes permits rapid functional analysis and reveals deletion mutants in immunosuppressed patients. J Virol 69: 5437–5444.
12. Sugauchi F, Orito E, Ichida T, Kato H, Sakugawa H, et al. (2003) Epidemiologic and virologic characteristics of hepatitis B virus genotype B having the recombination with genotype C. Gastroenterology 124: 925–932.
13. Martin D, Rybicki E (2000) RDP: detection of recombination amongst aligned sequences. Bioinformatics 16: 562–563.
14. Heath L, van der Walt E, Varsani A, Martin DP (2006) Recombination patterns in aphthoviruses mirror those found in other picornaviruses. J Virol 80: 11827–11832.
15. Worobey M, Holmes EC (1999) Evolutionary aspects of recombination in RNA viruses. J Gen Virol 80 (Pt 10): 2535–2543.
16. Abdou CM, Brichler S, Mansour W, Le Gal F, Garba A, et al. (2010) A novel hepatitis B virus (HBV) subgenotype D (D8) strain, resulting from recombination between genotypes D and E, is circulating in Niger along with HBV/E strains. J Gen Virol 91: 1609–1620.
17. Phung TB, Alestig E, Nguyen TL, Hannoun C, Lindh M (2010) Genotype X/C recombinant (putative genotype I) of hepatitis B virus is rare in Hanoi, Vietnam–genotypes B4 and C1 predominate. J Med Virol 82: 1327–1333.
18. Fang ZL, Hue S, Sabin CA, Li GJ, Yang JY, et al. (2011) A complex hepatitis B virus (X/C) recombinant is common in Long An county, Guangxi and may have originated in southern China. J Gen Virol 92: 402–411.
19. Mahgoub S, Candotti D, El EM, Allain JP (2011) Hepatitis B virus (HBV) infection and recombination between HBV genotypes D and E in asymptomatic blood donors from Khartoum, Sudan. J Clin Microbiol 49: 298–306.
20. Hannoun C, Norder H, Lindh M (2000) An aberrant genotype revealed in recombinant hepatitis B virus strains from Vietnam. J Gen Virol 81: 2267–2272.
21. Banner LR, Lai MM (1991) Random nature of coronavirus RNA recombination in the absence of selection pressure. Virology 185: 441–445.
22. Kato H, Orito E, Gish RG, Sugauchi F, Suzuki S, et al. (2002) Characteristics of hepatitis B virus isolates of genotype G and their phylogenetic differences from the other six genotypes (A through F). J Virol 76: 6131–6137.

23. Sugiyama M, Tanaka Y, Kato T, Orito E, Ito K, et al. (2006) Influence of hepatitis B virus genotypes on the intra- and extracellular expression of viral DNA and antigens. Hepatology 44: 915–924.
24. Sugiyama M, Tanaka Y, Sakamoto T, Maruyama I, Shimada T, et al. (2007) Early dynamics of hepatitis B virus in chimeric mice carrying human hepatocytes monoinfected or coinfected with genotype G. Hepatology 45: 929–937.
25. Yang J, Xing K, Deng R, Wang J, Wang X (2006) Identification of Hepatitis B virus putative intergenotype recombinants by using fragment typing. J Gen Virol 87: 2203–2215.
26. Tran TT, Trinh TN, Abe K (2008) New complex recombinant genotype of hepatitis B virus identified in Vietnam. J Virol 82: 5657–5663.
27. Simmonds P, Midgley S (2005) Recombination in the genesis and evolution of hepatitis B virus genotypes. J Virol 79: 15467–15476.
28. Morozov V, Pisareva M, Groudinin M (2000) Homologous recombination between different genotypes of hepatitis B virus. Gene 260: 55–65.
29. Owiredu WK, Kramvis A, Kew MC (2001) Hepatitis B virus DNA in serum of healthy black African adults positive for hepatitis B surface antibody alone: possible association with recombination between genotypes A and D. J Med Virol 64: 441–454.
30. Kurbanov F, Tanaka Y, Fujiwara K, Sugauchi F, Mbanya D, et al. (2005) A new subtype (subgenotype) Ac (A3) of hepatitis B virus and recombination between genotypes A and E in Cameroon. J Gen Virol 86: 2047–2056.
31. Tran TT, Trinh TN, Abe K (2008) New complex recombinant genotype of hepatitis B virus identified in Vietnam. J Virol 82: 5657–5663.
32. Tatematsu K, Tanaka Y, Kurbanov F, Sugauchi F, Mano S, et al. (2009) A genetic variant of hepatitis B virus divergent from known human and ape genotypes isolated from a Japanese patient and provisionally assigned to new genotype J. J Virol 83: 10538–10547.
33. Sugauchi F, Orito E, Ichida T, Kato H, Sakugawa H, et al. (2002) Hepatitis B virus of genotype B with or without recombination with genotype C over the precore region plus the core gene. J Virol 76: 5985–5992.

J Gastroenterol
DOI 10.1007/s00535-012-0596-x

ORIGINAL ARTICLE—LIVER, PANCREAS, AND BILIARY TRACT

Sequential immunological analysis of HBV/HCV co-infected patients during Peg-IFN/RBV therapy

Yasuteru Kondo · Yoshiyuki Ueno · Masashi Ninomiya · Keiichi Tamai · Yasuhito Tanaka · Jun Inoue · Eiji Kakazu · Koju Kobayashi · Osamu Kimura · Masahito Miura · Takeshi Yamamoto · Tomoo Kobayashi · Takehiko Igarashi · Tooru Shimosegawa

Received: 29 August 2011 / Accepted: 28 March 2012

Abstract

Background The immunopathogenesis of dual chronic infection with hepatitis B virus and hepatitis C virus (HBV/HCV) remains unclear. The in vivo suppressive effects of each virus on the other have been reported. In this study we aimed to analyze the virological and immunological parameters of HBV/HCV coinfected patients during pegylated interferon/ribavirin (Peg-IFN/RBV) therapy.

Methods One patient with high HBV-DNA and high HCV-RNA titers (HBV-high/HCV-high) and 5 patients with low HBV-DNA and high HCV-RNA titers (HBV-low/HCV-high) were enrolled. Twenty patients monoinfected with HBV and 10 patients monoinfected with HCV were enrolled as control subjects.. In vitro cultures of Huh 7 cells with HBV/HCV dual infection were used to analyze the direct interaction of HBV/HCV.

Results Direct interaction of HBV clones and HCV could not be detected in the Huh-7 cells. In the HBV-high/HCV-high-patient, the HCV-RNA level gradually declined and HBV-DNA gradually increased during Peg-IFN/RBV therapy. Activated CD4- and CD8-positive T cells were increased at 1 month of Peg-IFN/RBV-therapy, but HBV-specific IFN-γ-secreting cells were not increased and HBV-specific interleukin (IL)-10 secreting cells were increased. The level of HBV- and HCV-specific IFN-γ-secreting cells in the HBV-high/HCV-high-patient was low in comparison to that in the HBV- or HCV-monoinfected patients. In the HBV-low/HCV-high-patient, HCV-RNA and HBV-DNA rapidly declined during Peg-IFN/RBV therapy. Activated CD4- and CD8-positive T cells were increased, and HBV- and HCV-specific IFN-γ-secreting cells were also increased during Peg-IFN/RBV-therapy.

Conclusion The immunological responses of the HBV-high/HCV-high patient were low in comparison to the responses in HBV and HCV monoinfected patients. Moreover, the response of immune cells in the HBV-high/HCV-high patient during Peg-IFN/RBV therapy was insufficient to suppress HBV and HCV.

Keywords Dual infection · HBV · HCV · Immunopathogenesis

Electronic supplementary material The online version of this article (doi:10.1007/s00535-012-0596-x) contains supplementary material, which is available to authorized users.

Y. Kondo · Y. Ueno (✉) · M. Ninomiya · K. Tamai · J. Inoue · E. Kakazu · O. Kimura · T. Shimosegawa
Division of Gastroenterology, Tohoku University Graduate School of Medicine, 1-1 Seiryo, Aobaku, Sendai, Miyagi, Japan
e-mail: y-ueno@med.id.yamagata-u.ac.jp; yeuno@med.tohoku.ac.jp

Y. Tanaka
Virology and Liver Unit, Nagoya City University Medical School, Nagoya, Japan

K. Kobayashi
Tohoku University Graduate School of Medicine, 2-1 Seiryo, Aobaku, Sendai, Miyagi, Japan

M. Miura
Department of Gastroenterology, South Miyagi Medical Center, Oogawara, Miyagi, Japan

T. Yamamoto
Department of Gastroenterology, Tohoku Kosei-Nenkin Hospital, Sendai, Miyagi, Japan

T. Kobayashi
Department of Hepatology, Tohoku Rosai Hospital, Sendai, Miyagi, Japan

T. Igarashi
Department of Gastroenterology, Osaki Citizen Hospital, Osaki, Japan

Published online: 16 May 2012

Introduction

Hepatitis B virus (HBV) and Hepatitis C virus (HCV) are noncytopathic viruses that cause chronic hepatitis and hepatocellular carcinoma (HCC) [1, 2]. HBV now affects more than 400 million people worldwide, and persistent infection develops in ~5 % of adults and 95 % of neonates who become infected with HBV [3]. HCV infects about 170 million people worldwide and is a major cause of chronic hepatitis, cirrhosis, and HCC [4]. Some groups have mentioned that dual infection with HBV/HCV is not uncommon in Asian patients [5, 6]. The prevalence of patients with dual HBV/HCV infection is approximately 10–15 %, although it likely differs among countries [7–9]. Co-infection with HBV/HCV has been associated with severe liver disease and frequent progression to cirrhosis [10]. Moreover, a significantly higher incidence of HCC and liver-related mortality was noted in patients with HBV/HCV co-infection [11, 12]. However, some groups reported, based on a meta-analysis, that dual infection with HBV/HCV did not increase the risk of HCC [13, 14]. These contradictory reports could be explained by the rarity of dual infection with HBV/HCV in patients without clinically evident liver disease. It might be difficult to estimate the hepatocarcinogenic risk of dual infection compared with that of either infection alone in such clinical settings [15].

An inverse relationship in the replicative levels of the two viruses has been noted, suggesting direct or indirect effects in vivo [16]. More recently, some groups have reported, using an in vitro infection system, that there is little direct interaction of HBV/HCV in coinfected hepatocytes [17, 18]. Therefore, the viral interference observed in coinfected patients is probably due to indirect mechanisms mediated by the innate and/or adaptive host immune responses.

The cellular immune response to HBV and HCV plays an important role in the pathogenesis of chronic hepatitis, cirrhosis, and HCC [19–21]. Hyporesponsiveness of HBV- or HCV-specific T-helper 1 cells and excessive regulatory function of $CD4^+CD25^+FoxP3^+$ regulatory T cells (Tregs) in peripheral blood have been shown in patients with chronic hepatitis B and C [22–34]. Recently, we reported that HBV replication stress could enhance the suppressive activity of Tregs via TLR2 [35]. However, little is known about the immunopathogenesis of HBV/HCV dual infection.

Dual infection can be classified into several groups (e.g., group A: HBV active and HCV active; group B: HBV inactive and HCV active; and group C: HBV active and HCV inactive) [36]. HCV is reported to be the dominant virus in HBV/HCV dual infection, but the dominance of either virus might be due to the genotypes of each virus and/or ethnic differences that could affect the proliferative activity of the viruses [36]. In this study, we investigated immunopathogenesis in a group A patient and in group B patients during therapy with pegylated interferon-α2b (Peg-IFN-α2b) plus ribavirin.

Patients, materials, and methods

Patients

One patient with high HBV-DNA and high HCV-RNA titers (HBV-high/HCV-high; patient A) and 5 patients with low HBV-DNA and high HCV-RNA titers (HBV-low/HCV-high) were enrolled (one of these patients, whose results were analyzed in detail, was termed patient B; see findings below in the "Results"). Twenty patients monoinfected with HBV and 10 patients monoinfected with HCV were enrolled as control subjects. None of the patients had liver disease due to other causes, such as alcohol, drugs, congestive heart failure, or autoimmune diseases. Permission for the study was obtained from the Ethics Committee at Tohoku University Graduate School of Medicine (permission no. 2006-194). Written informed consent was obtained from all the participants enrolled in this study. Participants were monitored for two years. At each assessment, patients were evaluated by biochemical laboratory tests, immunological analysis, and virological tests. Liver histology was analyzed at the start of Peg-IFN/RBV therapy by using laparoscopic liver biopsy samples and by employment of the METAVIR score.

Detection of interleukin (IL)-28B polymorphism

Genomic DNA was isolated from peripheral blood mononuclear cells (PBMCs) using an automated DNA isolation kit. Then polymorphism of IL-28B (rs8099917) was analyzed using real-time polymerase chain reaction (PCR) (TaqMan SNP Genotyping Assay, Applied Biosystems, CA, USA). Detection of the IL-28B polymorphism was approved by the Ethics Committee at Tohoku University Graduate School of Medicine (permission no. 2010-323).

Isolation of peripheral blood mononuclear cells (PBMCs) and flow cytometry

Peripheral blood mononuclear cells (PBMCs) were isolated from fresh heparinized blood by means of Ficoll-Hypaque density gradient centrifugation (Amersham Bioscience, Uppsala, Sweden). PBMCs were stained with CD3, CD4, CD8, CD19, CD25, CD40, CD56, CD86, HLA-DR, NKG2D, and isotype control antibodies (Becton Dickinson, NJ, USA) for 15 min on ice to analyze the frequency